Photosensitivity of Ga_2O_3 Schottky Diodes: Effects of Deep Acceptor Traps Present before and after Neutron Irradiation

E.B. Yakimov[1, 2], A.Y. Polyakov[2], I.V. Shchemerov[2], N.B. Smirnov[2], A.A. Vasilev[2], P.S. Vergeles[1], E.E. Yakimov[1], A.V. Chernykh[2], A. S. Shikoh[2], F. Ren[3] and S.J. Pearton[4*]

[1]Institute of Microelectronics Technology and High Purity Materials, Russian Academy of Sciences, Moscow Region 142432, Russia

[2]National University of Science and Technology MISiS, Moscow 119049, Russia

[3] Department of Chemical Engineering, University of Florida, Gainesville, FL 32611 USA

[4]Department of Materials Science and Engineering, University of Florida, Gainesville, FL 32611 USA

*Corresponding author, E-mail: spear@mse.ufl.edu

Photocurrent produced by 259 nm wavelength excitation was measured in β-Ga_2O_3 Schottky diodes before and after neutron irradiation. These samples differed by the density of deep acceptors in the lower half of the bandgap as detected by capacitance-voltage profiling under monochromatic illumination. Irradiation led to a very strong increase of photocurrent, which closely correlated to the increase of deep trap density and the decrease after illumination of the effective Schottky barrier height due to hole capture by acceptors. A similar effect was observed on as-grown βs-Ga_2O_3 film with a high density of deep acceptors. Electron beam induced current measurements indicated a strong amplification of photocurrent, which is attributed to the Schottky barrier lowering by holes trapped on acceptors near the surface. Photocurrent build-up and decay curves show several time constants ranging from several milliseconds to many seconds. These characteristic times are attributed to electrons tunneling into the hole-filled acceptors near the surface and to thermal emission of holes from deep acceptors.

The transparent wide-bandgap semiconductor Ga_2O_3 has excellent potential for applications in power electronics [1,2] and solar-blind photodetectors [2-4]. In the latter case, the advantage is due to the bandgap close to 5 eV, rendering photodetectors based on Ga_2O_3 to only be sensitive to photons in the far-UV spectral range and also exhibit a high photosensitivity of Ga_2O_3 detectors. There have been many recent reports on photoresponse properties of Ga_2O_3 photodetectors, both for the interdigital back-to-back Schottky diodes architecture operation at high applied voltages and for simple Schottky diode architectures both in photovoltaic and in biased modes [3-12]. Many of these report extremely high external quantum efficiency (EQE) of photoresponse, often exceeding hundreds or even thousands percent [3-12]. To explain such high EQE values in Ga_2O_3-based Schottky diodes, impact ionization amplification [5,6, 8], modulation of Schottky barrier height by self-trapped polaronic hole states (STH) [7] or by hole accumulation near the Schottky metal [3] have been proposed.

However, the electric field strength in all reported experiments is far short of the impact ionization threshold of around 5-8 MV/cm [1, 2, 13] estimated for β-Ga_2O_3. As for STH-related charge accumulation in Ga_2O_3 Schottky diodes, it has been shown recently that above ~140 K and certainly at room temperature, mobile holes rather than STH polaronic states are dominant and mainly contribute to the formation of photocurrent or electron beam induced current (EBIC) [14-17]. At the same time, it is well known that a variety of deep hole traps in the lower half of the bandgap can be formed in Ga_2O_3 and give rise to significant hole trapping in the space charge region [18] with potentially a similar effect on the Schottky barrier height and photocurrent EQE as the STH states proposed in Ref. [7]. In a recent paper on EBIC collection efficiency in β-Ga_2O_3 [17] it was reported that an increased hole trap concentration favored a better collection efficiency. One would expect that similar beneficial effects should be observed for photocurrent and possibly lead to high photocurrent EQE. To check this assumption, we performed photocurrent and EBIC measurements on β-Ga_2O_3 Schottky diodes vastly differing in their density of deep hole traps. These experiments convincingly show the photosensitivity of β-Ga_2O_3

Schottky diode detectors increases with increased density of deep hole traps in the lower half of the bandgap. This helps suggest how the photosensitivity of such detectors can be improved.

The samples studied in this work were acquired from Tamura/Novel Crystals Technology (Japan). They were grown by halide vapor phase epitaxy (HVPE) on bulk substrates grown by Edge-Defined Film-Fed Growth (EFG). The orientation of the substrates according to the manufacturer's specification was (010). The HVPE films were doped with Si, with starting shallow donor concentration for one sample 1.3×10^{16} cm^{-3}, and 1.1×10^{17} cm^{-3} for the other. The substrates were doped with Sn to net donor concentration of 3×10^{18} cm^{-3}. The thickness of the HVPE films was 10 μm and the substrate thickness was 650 μm. For the lower doped HVPE film, three pieces were studied, one before neutron irradiation (called henceforth Sample1), and two after neutron irradiation with fast neutron fluences of respectively 5×10^{13} cm^{-3} (Sample1_5E13) and 4×10^{14} cm^{-3} (Sample1_4E14). Irradiation was done using a two-zone pulsed self-extinguishing fast-neutron reactor BARS-6 [19]. For these three samples, net donor concentrations from capacitance-voltage (C-V) profiling, deep electron trap spectra from deep level transient spectroscopy DLTS [20], and deep hole trap spectra from C-V profiling under monochromatic light illumination (LCV)[21, 22] were measured [19]. The net donor concentration decreased from 1.3×10^{16} cm^{-3} in the virgin Sample1 to 5.3×10^{15} cm^{-3} in Sample1_4E14. In deep electron trap spectra, the E2 traps near E_c-0.8 eV related to Fe acceptors [23-25] and native-defects- related E2* (E_c-0.75 eV), E3 (E_c-1 eV), and E4 (E_c-1.2 eV) [26] traps were detected. The concentration of the dominant E2 traps was 2×10^{14} cm^{-3} for all samples, while the concentrations of other traps increased with neutron fluence from low 10^{13} cm^{-3} in Sample1 to 1.5×10^{14} cm^{-3} in Sample1_4E14 [19]. The main deep acceptor traps detected in LCV spectra had optical ionization thresholds close to 2.3 eV and 3.1 eV, both associated in the literature with Ga vacancy acceptor related defects [19].

The properties of traps in the S2 sample have been reported elsewhere [17]. The concentration profile of this sample calculated from C-V data, the spectral dependence of

photoconcentration ΔN_{ph} obtained from LCV data, electron traps DLTS spectra for this sample are shown in Fig. 1S, 2S, 3S of the Supplementary material. In sample S2, the dominant electron trap is the E2 Fe-related center with concentration of 7×10^{15} cm^{-3}, and a lower concentration of 1.5×10^{15} cm^{-3} E3 traps. The types of deep acceptor traps in LCV spectra were similar to those in Sample1, but the concentrations were about an order of magnitude higher. For the subject of this paper, the variations in the density of deep hole traps are of most importance. Respective values are presented in Table I.

For all samples, transparent front surface Ni Schottky diodes with diameter of 1.2 mm and metal thickness of 20 nm were prepared by electron beam evaporation through a shadow mask. The back Ohmic contacts were made by Ti/Au electron beam evaporation on the substrate side surface preliminarily subjected to Ar plasma treatment and subsequent rapid thermal annealing at 300°C [27]. For neutron irradiation the Ohmic contacts were prepared before irradiation, while the Schottky diodes were deposited after irradiation. Current-voltage (I-V) characteristics were measured in the dark and under illumination using two- channel B2902A voltage/current source/meter (Keysight Technologies, USA). For illumination, GaN-based light emitting diodes with peak wavelength of 259 nm (QPhotonics LLC, USA) were used. Three LEDs were bunched together and connected in series, to produce a light spot of 5 mm in diameter with maximum optical output density within this 5 mm spot of 5×10^{-4}W/cm^{2}. Dark I-V measurements were performed at different temperatures from 100-460K to determine the ideality factor and saturation current in the forward direction and estimate the Schottky barrier height. C-V measurements in the dark, under 259 nm illumination, and after illumination were done using E4980A LCR meter (KeySight Technologies, USA, frequency range 20Hz-1 MHz).

The EBIC measurements were carried out at 300K in a scanning electron microscope JSM-840A (JEOL, Japan) using a Keithley 428 current amplifier to measure the beam current I_b and the EBIC current I_c at the beam energy E_b. In these experiments, the value of EBIC current I_c normalized by the product of the beam energy E_b and the beam current I_b, $I_c/(I_b\times E_b)$, was

measured as a function of the bias applied to the Schottky diode and of beam energy. This was then compared to theoretical predictions based on calculating the beam penetration depth and the spatial distribution of the electron-hole generation function [15, 17]. After switching off the excitation, the dark current was larger than before excitation and slowly decayed to the initial value. To minimize this effect, the Schottky barrier was irradiated with an e-beam pulse of 1.5 s duration and small beam currents, with values chosen to obtain measurable induced current.

We also monitored the kinetics of photocurrent build-up and decay with step-wise illumination with the 259 nm LED. The photocurrent transients were measured using the B2902A meter, with a time step of 0.2 ms up to times of 30-60 s. The measurements were performed from 300- 400K, with the temperature stabilized with accuracy better than 0.1K. Fig. 4S of the Supplementary material also shows the room temperature micro-cathodoluminescence (MCL) spectra of the samples.

Dark I-V characteristics of all samples showed good ideality in the forward direction, with the ideality factor close to 1 and saturation current in the forward direction showing activation energy 1.05-1.1 eV, corresponding to the Schottky barrier height (actual data presented in Supplementary Material). In reverse direction, the current showed a measurable dependence on voltage and a slight temperature dependence with effective activation energy ~0.3 eV, suggesting tunneling assisted current flow involving traps. The 300K reverse I-V characteristics in the dark and with 259 nm LED illumination are shown for samples S1, S1_5E13, S1_5E14 in Fig. 1. The photocurrent markedly increases with neutron irradiation dose and with applied voltage. For reverse voltage of -60V, the photocurrent increased by 2.5 times after irradiation with 5×10^{13} cm^{-2} neutrons and by 18 times for 4×10^{14} cm^{-2} neutrons compared with the virgin sample S1. For sample S2, the photocurrent measurements could only be done up to -40V, but at this lower voltage the photocurrent density was 0.02A/ cm^2, i.e. almost a 1000 times higher than for sample S1 (data can be found in the Supplementary Material).

The EBIC collection efficiency dependence on applied voltage for samples S1, S2, and S1_4E14 is shown in Fig. 2. The measurements were done with beam electron energy of 4 kV, which generates charge carriers down to a depth of 50 nm from the surface, i.e. well within the space charge region of the Schottky diode [17]. Under these conditions, normally the entire charge of the generated electron-hole pairs should be fully collected and the calculated normalized value of the EBIC signal $I_c/(I_b x E_b)$ should be close to 15 keV^{-1} and should not depend on voltage until the onset of the charge multiplication caused by the band-to-band impact ionization or the impact ionization of deep traps [17]. This is approximately the case for Sample1 up to a voltage of 150V, when the signal starts to increase (the voltage corresponds to the maximal electric field in the diode close to 10^6 V/cm). After irradiation with 4×10^{14} n/cm^2 neutrons, the normalized EBIC signal at high applied voltages is about an order of magnitude higher than expected, while for the S2 sample the actual signal is orders of magnitude higher than predicted.

This discrepancy suggests the existence of a multiplication mechanism. The bulk impact ionization can be excluded because the electric field strength for which amplification is observed in our samples does not exceed 10^6 V/cm, i.e. far short of predicted values of 5-8 MV/cm [2, 13]. Another option is the photocurrent amplification driven by lowering of the Schottky barrier height by the excessive charge localized near the metal interface [7]. In Ref. [7] it was proposed that the phenomenon is related to polaronic self-trapped holes, but positive charge accumulation on deep acceptor states should lead to similar effect. In Fig. 3 we show the charge concentration profiles deduced for samples S1, S1_5E13, and S1_4E14 from C-V profiling in the dark and under 259 nm LED illumination. A considerable increase of the charge concentration occurs down to ~1 μm from the surface upon illumination. The holes trapped on the deep centers below the Fermi level should change the apparent Schottky barrier height. Solving the Poisson equation yields the decrease of the apparent barrier height as $\Delta V_{bi}=N_{deep}\times q\times w_o^2/(2\varepsilon\varepsilon_o)$ [28], where N_{deep} is the density of deep traps that have been recharged, w_o is the depth to which the traps have

been recharged during illumination, q is the electronic charge, ε_0 is the dielectric constant of vacuum, and ε is the relative dielectric constant.

The effect manifests itself in the decrease of the voltage offset in the $1/C^2$ versus V plots measured in the dark and after illumination by ΔV_{bi} [28]. Fig. 4 shows such C-V plots measured at 300K before and after illumination with the 259 nm LED for sample S1_4E14. Before illumination, the voltage offset is 1.03 V giving a barrier height close to that obtained from I-V measurements. After illumination, the voltage offset decreased by 0.15 V because of the charge of holes trapped on deep acceptors. The density of charge trapped on deep acceptors estimated from this ΔV_{bi} shift is ~ 8×10^{14} cm^{-3} and similar to the density of deep hole traps determined from LCV profiling in Ref. [19] and presented in Table I. For other samples, the changes in the barrier height caused by trapping during illumination are presented in Table I. In a simple approach, these changes in the barrier height should convert themselves into the exponential increase of the current flowing through the Schottky diode. Fig. 5 shows this increase in current for samples S1, S1_5E13, and S1_4E14 (the results are normalized to the value for sample S1). The amount of increase in the samples photocurrent is qualitatively similar to the actual changes in photocurrent with increased density of deep acceptor traps and at least, in part, explains the observed multiplication of the signal in photocurrent measurements.

There is, however, a problem related to the proposed mechanism, in terms of the disposal of the charge accumulated on deep acceptors. The depth of the centers is quite high and thermal emission of holes captured during illumination should be very slow at room temperature and strongly depend on temperature. The actual times of photocurrent build-up and decay in Ga_2O_3 photodetectors [3] are indeed quite long, many seconds to minutes. However, the waveform of the transient photocurrent and the effects of temperature on characteristic times are generally not reported.

The results of actual measurements performed for the S1 and S1_4E14 samples of the present set (Fig. 6 shows the data for Sample1_4E14, in the Supplementary material we present

the same data on a shorter time scale and similar data for Sample 1) show that: a) the build-up and decay times are indeed very long, many seconds, b) the photocurrent transients cannot be represented as single exponents, but rather consist of several exponential decays for which the shortest decay time is close to 100 ms and very weakly depends on temperature, while for longer times, several other decay processes take place with much longer time constants that become shorter with increased temperature. These longer decay times could be related to deep hole traps emitting holes thermally whilst the short decay time weakly dependent on temperature could be due to electrons tunneling from the metal contact into the deep trap states filled with holes.

While a more detailed understanding of the mechanisms involved is needed, our current model summarized by Fig. 7 is as follows: Electrons and holes are produced in the space charge region by illumination, holes slowly drift to the metal contact and on the way are captured by deep hole traps, thus varying the built-in charge and lowering the Schottky barrier height, the main cause of high gain in photocurrent. The photocurrent decay occurs by tunneling of electrons from the metal into the acceptor states filled with holes near the metal and by thermal emission of holes deeper in the material. The hole trap states closest to the surface should be most significant in varying the Schottky barrier height. This explains the marked dependence of the photocurrent on applied voltage, since holes in Ga_2O_3 are heavy and a high electric field is necessary to accelerate them and efficiently deliver them close to the surface.

In summary, the photocurrent in β-Ga_2O_3 Schottky diodes can be strongly enhanced when the density of deep hole traps in the lower half of the bandgap is increased. The effect is attributed to holes accumulation on these acceptors giving rise to the increased space charge density near the surface leading to a decrease of the Schottky barrier height and corresponding photocurrent amplification. The efficiency of the process is boosted by increasing the electric field in the space charge region to increase the hole velocity and facilitates their delivery to the near-surface region where the local charge build-up is most conducive to the decrease in Schottky barrier height. The photocurrent decay is provided by electrons tunneling into the deep

acceptor states filled with holes near the surface and by thermal emission of holes from deep acceptors that are further removed from the surface. This explains the unusually long photocurrent build-up and decay times commonly observed in β-Ga_2O_3 Schottky diodes [3]. This peculiar mechanism of photocurrent flow in β-Ga_2O_3 Schottky diodes explains the unexpected increase in photocurrent of such diodes after irradiation. Understanding this mechanism also suggests approaches to improving the photosensitivity of β-Ga_2O_3 Schottky diodes. Specifically, since most of the deep acceptors in the lower half of the bandgap are attributed to defects related to Ga vacancy acceptors [16, 26] the photosensitivity is expected to be increased by treatments enhancing the density of Ga vacancies: growth in O-rich conditions, high-energy particle irradiations that increase the density of Ga vacancies [19, 26], surface treatment in ozone (reported to be beneficial for photosensitivity [3]), high-energy plasma treatment shown to generate defects in the lower half of the bandgap of gallium oxide [29].

Supplementary Material

See supplementary material for the detailed materials properties of the Ga_2O_3 structures used in these experiments.

ACKNOWLEDGMENTS

The work at NUST MISiS was supported in part by Grant № K2-2020-011 under the Program to increase Competitiveness of NUST MISiS among the World Leading Scientific and Educational centers (Program funded by the Russian Ministry of Science and Education). The work at IMT RAS was supported in part by the State Task No 075-00920-20-00. The work at UF was sponsored by Department of the Defense, Defense Threat Reduction Agency, HDTRA1-17-1-011, monitored by J. Calkins, DTRA Interaction of Ionizing Radiation with Matter University Research Alliance, HDTRA1-19-S-0004 (Jacob Calkins) and also by NSF DMR 1856662 (James Edgar).

Data Availability

The data that supports the findings of this study are available within the article [and its supplementary material].

REFERENCES

[1] S. J. Pearton, Fan Ren, Marko Tadjer, and Jihyun Kim, Perspective: Ga_2O_3 for ultra-high power rectifiers and MOSFETS, J. Appl. Phys. 124, 220901 (2018)

[2] S. J. Pearton, J. Yang, P. H. Cary, F. Ren, Jihyun Kim, M. J. Tadjer, and M. A. Mastro, A review of Ga_2O_3 materials, processing and devices, Appl. Phys. Rev. 5, 011301 (2018)

[3] J. Xu, W. Zheng and F. Huang. Gallium oxide solar-blind ultraviolet photodetectors: a review. J. Mater. Chem. C, 7, 8753 (2019)

[4] X. Chen, F. Ren, S. Gu, J. Ye. Review of gallium-oxide-based solar-blind ultraviolet photodetectors. Photonics Research, 7, 381-415, 2019

[5] G. C. Hu, C. X. Shan, Nan Zhang, M. M. Jiang, S. P. Wang, D. Z. Shen. High gain Ga_2O_3 solar-blind photodetectors realized via a carrier multiplication process. Optics Express 23, 13554, 2015

[6] B. Qiao, Z. Zhang, X. Xie, B. Li, Kexue Li, Xing Chen, Haifeng Zhao, Kewei Liu, Lei Liu, Dezhen Shen. Avalanche Gain in Metal−Semiconductor−Metal Ga_2O_3 Solar-Blind Photodiodes. J. Phys. Chem. C 123, 18516 (2019)

[7] A.M Armstrong, M.H. Crawford, A. Jayawardena, A. Ahyi and S. Dhar, Role of self-trapped holes in the photoconductive gain of β-Ga_2O_3 Schottky diodes, Appl. Phys. 119 103102 (2016)

[8] Sooyeoun Oh,1 Hyoung Woo Kim,2 and Jihyun Kim, High Gain β-Ga2O3 Solar-Blind Schottky Barrier Photodiodes via Carrier Multiplication Process, ECS J. Sol. State Sci. Technology, 7, Q196 (2018)

[9] Y. Qin, L. Li, X. Zhao, G.S. Tompa, H. Dong, G. Jian, Q. He, P. Tan, X. Hou, Z. Zhang, S. Yu, H. Sun, G. Xu, X. Miao, K. Xue, S. Long, M. Liu. Metal−Semiconductor−Metal ε-Ga_2O_3 Solar-Blind Photodetectors with a Record-High Responsivity Rejection Ratio and Their Gain Mechanism. ACS Photonics, 7, 812 (2020).

[10] X. Chen, F.-F. Ren, J. Ye and S. Gu, Gallium oxide-based solar-blind ultraviolet Photodetectors. Semicond. Sci. Technol. 35,023001 (2020)

[11] Z.X. Jiang, Z.Y. Wu, C.C. Ma, J.N. Deng, H. Zhang, Y. Xu, J.D. Ye, Z.L. Fang, G.Q. Zhang, J.Y. Kang, T.-Y. Zhang. P-type β-Ga_2O_3 metal-semiconductor-metal solar-blind photodetectors with extremely high responsivity and gain-bandwidth product. Mater. Today Phys. 14 (2020) 100226

[12] Hyun Kim, Sergey Tarelkin, Alexander Polyakov, Sergey Troschiev, Sergey Nosukhin, Mikhail Kuznetsov, and Jihyun Kim, Ultrawide-Bandgap p-n Heterojunction of Diamond/β-Ga_2O_3 for a Solar-Blind Photodiode, ECS J. Solid State Sci. Technol, 9, 045004 (2020)

[13] K. Ghosh, U Singisetti. Impact ionization in β-Ga_2O_3. J. Appl. Phys. 124, 085707 (2018)

[14] A. Y. Polyakov, N. B. Smirnov, I. V. Shchemerov, S. J. Pearton, F. Ren, A. V. Chernykh, P. B. Lagov, and T. V.Kulevoy, Hole traps and persistent photocapacitance in proton irradiated -Ga2O3 films doped with Si, APL Materials 6, 096102 (2018)

[15] E. B. Yakimov, A. Y. Polyakov, N. B. Smirnov, I. V. Shchemerov, Jiancheng Yang, F. Ren, Gwangseok Yang, Jihyun Kim, and S. J. Pearton, Diffusion length of non-equilibrium minority charge carriers in β-Ga_2O_3 measured by electron beam induced current, Journal of Applied Physics 123, 185704 (2018)

[16] E B Yakimov and A Y Polyakov, Defects and carrier lifetimes in Ga_2O_3, in Wide Bandgap Semiconductor-Based Electronics, ed. Fan Ren and S. Pearton (IOP Publishers, 2020) chapter 5

[17] E.B. Yakimov, A.Y. Polyakov, N. B. Smirnov, I.V. Shchemerov, P.S. Vergeles, E.E. Yakimov, A.V. Chernykh, Minghan Xian, F. Ren, S.J. Pearton. Role of Hole Trapping by Deep Acceptors in Electron Beam Induced Current Measurements in β-Ga_2O_3 Vertical Rectifiers. J. Phys. D, (2020)

[18] Jihyun Kim, Stephen J. Pearton, Chaker Fares, Jiancheng Yang, Fan Ren, Suhyun Kim and Alexander Y. Polyakov, Radiation damage effects in Ga_2O_3 materials and devices, J. Mater. Chem. C, (2018)

[19] A. Y. Polyakov, N. B. Smirnov, I. V. Shchemerov, A. A. Vasilev, E. B, Yakimov, A. V. Chernykh, A. I. Kochkova, P. B. Lagov, Yu S. Pavlov, O. F. Kukharchuk, A. A. Suvorov, N. S.

Garanin, In-Hwan Lee, M. Xian, Fan Ren and S J Pearton, Pulsed fast reactor neutron irradiation effects in Si doped n-type β-Ga_2O_3, J. Phys. D: Appl. Phys. 53, 274001 (2020)

[20] Capacitance spectroscopy of semiconductors, ed. Jian V. Li and Giorgio Ferrari (Pan Stanford Publishing Pte Ltd, Singapore, 2018) 437 pp

[21] Z. Zhang, E. Farzana, A. R. Arehart, and , and S. A. Ringel, Deep level defects throughout the bandgap of (010) β-Ga_2O_3 detected by optically and thermally stimulated defect spectroscopy, Appl. Phys. Lett. 108, 052105 (2016)

[22] Esmat Farzana, Elaheh Ahmadi, James S. Speck, Aaron R. Arehart, and Steven A. Ringel, Deep level defects in Ge-doped (010) β-Ga2O3 layers grown by plasma-assisted molecular beam epitaxy, Journal of Applied Physics 123, 161410 (2018)

[23] Adam T. Neal, Shin Mou, Subrina Rafique, Hongping Zhao, Elaheh Ahmadi, James S. Speck, Kevin T. Stevens, John D. Blevins, Darren B. Thomson, Neil Moser, Kelson D. Chabak, and Gregg H. Jessen, Donors and deep acceptors in β-Ga_2O_3, Appl. Phys. Lett. 113, 062101 (2018)

[24] A. Y. Polyakov, N. B. Smirnov, I. V. Shchemerov, S. J. Pearton, Fan Ren, A. V. Chernykh, and A. I. Kochkova, Electrical properties of bulk semi-insulating β-Ga_2O_3 (Fe), Appl. Phys. Lett. 113, 142102 (2018)

[25] M. E. Ingebrigtsen, J. B. Varley, A. Yu. Kuznetsov, B. G. Svensson, G. Alfieri, A. Mihaila, U. Badstübner, and L.Vines, Iron and intrinsic deep level states in Ga_2O_3, Appl. Phys. Lett. 112, 042104 (2018).

[26] A. Y. Polyakov, N. B. Smirnov, I. V. Shchemerov, E. B. Yakimov, S. J. Pearton, Chaker Fares, Jiancheng Yang, Fan Ren, Jihyun Kim, P. B. Lagov, V. S. Stolbunov, and A. Kochkova, Defects responsible for charge carrier removal and correlation with deep level introduction in irradiated β-Ga_2O_3, Appl. Phys. Lett. 113, 092102 (2018)

[27] A.Y. Polyakov, N.B. Smirnov, I.V. Shchemerov, E.B. Yakimov, Jiancheng Yang, F. Ren, Gwangseok Yang, Jihyun Kim, A.Kuramata, and S. J. Pearton, Effect of 10 MeV Proton

Irradiation on Electrical Properties and Recombination in Ga_2O_3 Schottky Diodes, Appl. Phys. Lett., 112, 032107 (2018)

[28] A.Y. Polyakov and In-Hwan Lee, Deep traps in GaN-based structures as affecting the performance of GaN devices (a review), Mat. Sci& Eng. (R), 94, 1-56 (2015)

[29] A. Y. Polyakov, In-Hwan Lee, N. B. Smirnov, E. B. Yakimov, I. V. Shchemerov, A. V. Chernykh, A. I. Kochkova, A. A. Vasilev, P. H. Carey, F. Ren, D. J. Smith, and S. J. Pearton, Defects at the surface of β-Ga_2O_3 produced by Ar plasma exposure, APL Mater. **7**, 061102 (2019).

Table I. Net donor concentrations N_d, concentrations of deep hole traps with optical ionization energy of 2.3 eV (N (2.3 eV)), traps with optical ionization energy 3.1 eV (N (3.1 eV)), and the persistent change of the Schottky barrier height ΔV_{bi} in C-V characteristics after illumination with 259 nm LED

Sample #	N_d ($\times 10^{16}$ cm^{-3})	N (2.3 eV) ($\times 10^{14}$ cm^{-3})	N (3.1 eV) ($\times 10^{14}$ cm^{-3})	ΔV_{bi} (V)
S1	1.4	2	-	0.03
S1_5E13	1.2	3	1.1	0.09
S1_5E14	0.53	7.7	2.7	0.15
S2	11	20	20	0.35

FIGURE CAPTIONS

Fig. 1 (Color online) Room temperature dark reverse current and photocurrent under 259 nm LED illumination for three samples of β-Ga_2O_3 Schottky diodes

Fig. 2 (Color online) Normalized EBIC signal as a function of applied reverse bias for samples S1, S2, S1_4E14 with the probing beam electrons energy of 4 keV and the beam current of 12 pA

Fig. 3 (Color online) Dark (solid line) charge concentration profiles and profiles measured with 259 nm illumination for three β-Ga_2O_3 Schottky diode samples S1, S1_5E13, and S1_4e14

Fig. 4 (Color online) Room temperature $1/C^2$ versus V plots measured in the dark and after illumination with 259 nm LED for sample S1_4E14

Fig. 5. Changes expected in photocurrent for the Schottky barrier height of 1 eV assuming that the changes are caused by the change of the Schottky barrier height produced by charging the deep acceptor traps; the points correspond to the changes in ΔV_{bi} observed in samples S1, S1_5E13, and S1_4E14 after 259 nm LED illumination

Fig. 6 (Color online) Photocurrent build-up and decay curves for 300K and 400K for sample S1_4E14

Fig.7 (Color online) Schematic representation of the processes involved in photocurrent build-up and decay in β-Ga_2O_3 Schottky diodes

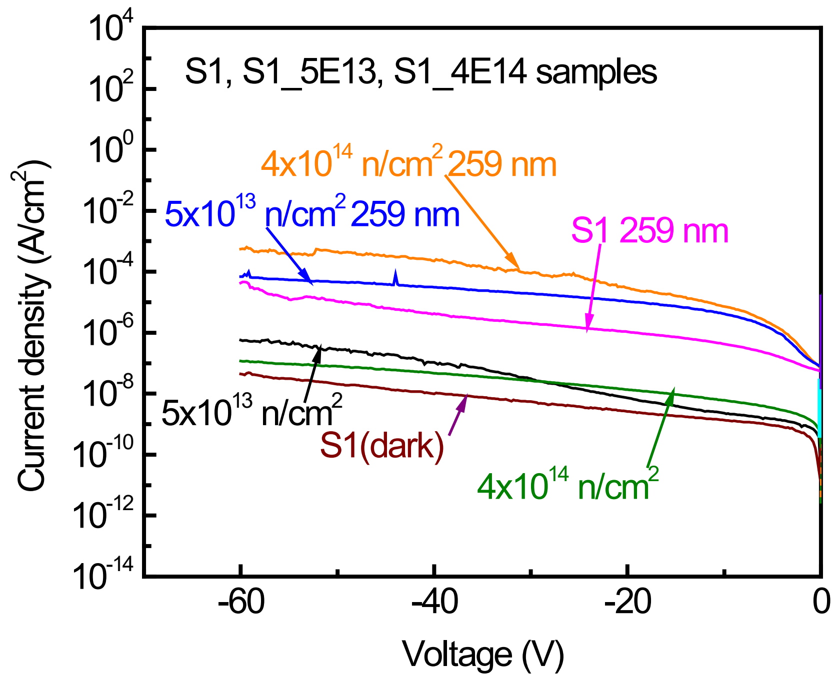

Fig. 1 (Color online) Room temperature dark reverse current and photocurrent under 259 nm LED illumination for three samples of β-Ga_2O_3 Schottky diodes

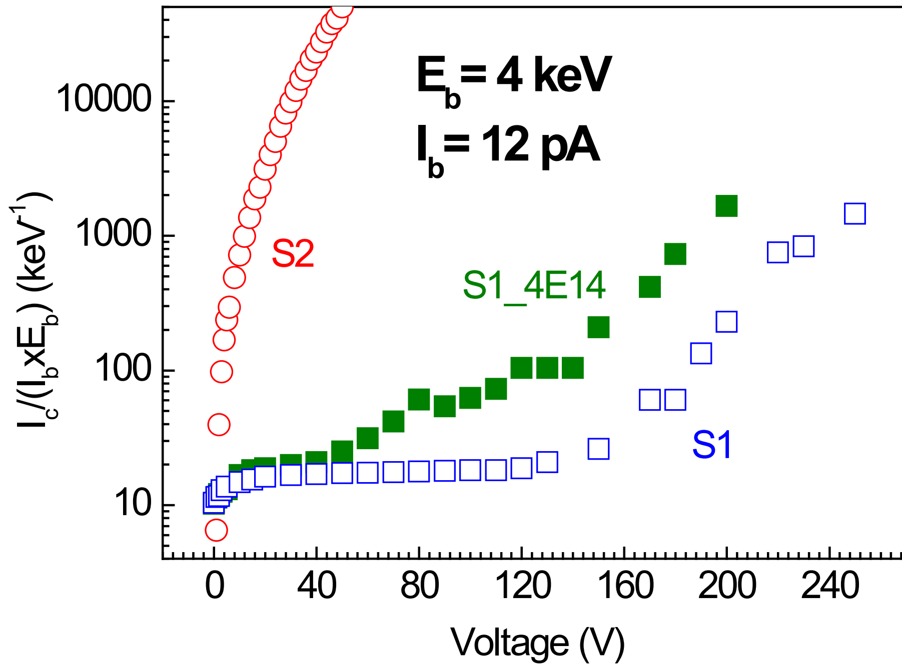

Fig. 2 (Color online) Normalized EBIC signal as a function of applied reverse bias for samples S1, S2, S1_4E14 with the probing beam electrons energy of 4 keV and the beam current of 12 pA

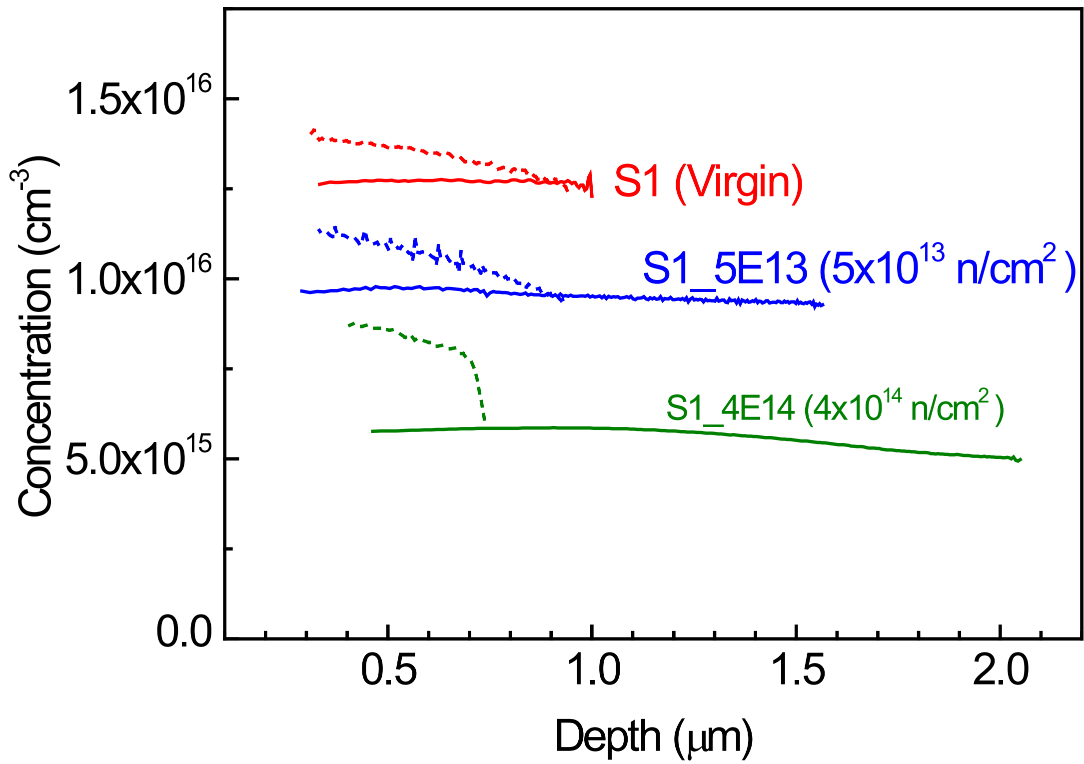

Fig. 3 (Color online) Dark (solid line) charge concentration profiles and profiles measured with 259 nm illumination (dashed line) for three β-Ga_2O_3 Schottky diode samples S1, S1_5E13, and S1_4e14

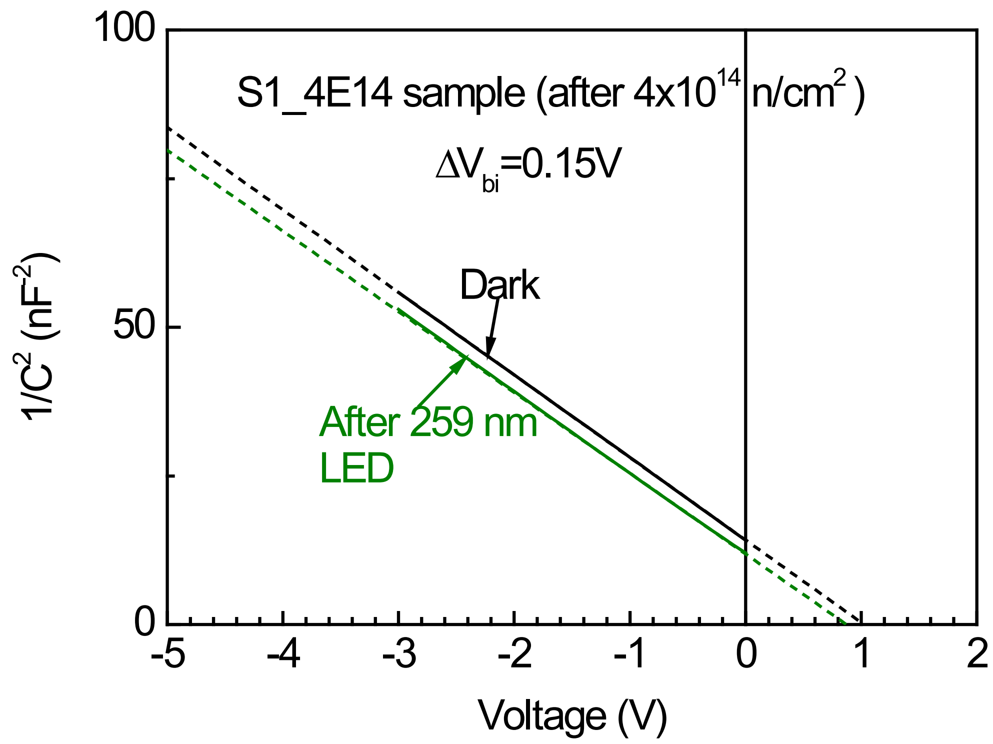

Fig. 4 (Color online) Room temperature $1/C^2$ versus V plots measured in the dark and after illumination with 259 nm LED for sample S1_4E14

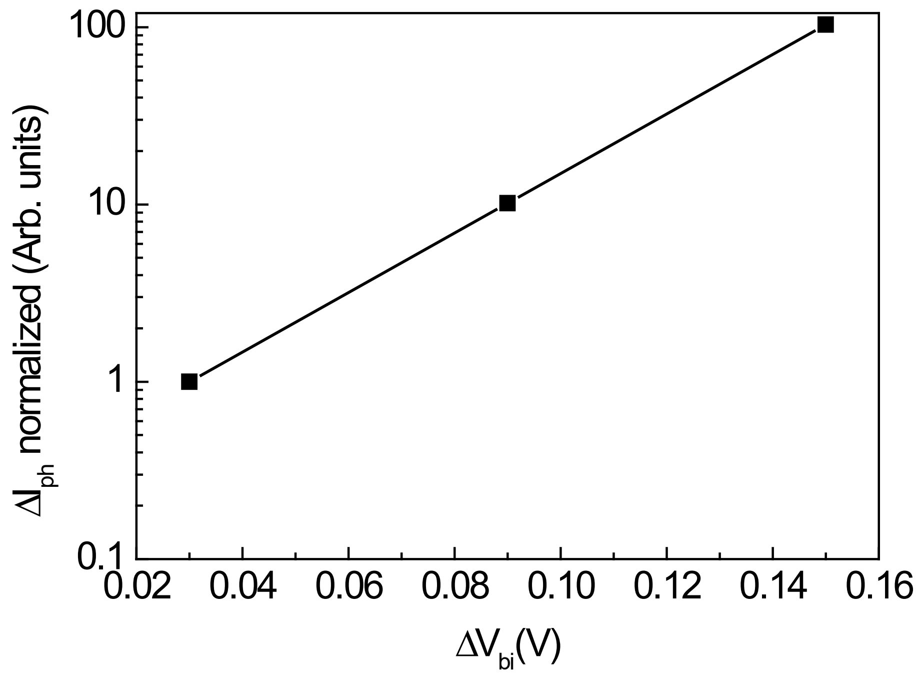

Fig. 5. Changes expected in photocurrent for the Schottky barrier height of 1 eV assuming that the changes are caused by the change of the Schottky barrier height produced by charging the deep acceptor traps; the points correspond to the changes in ΔV_{bi} observed in samples S1, S1_5E13, and S1_4E14 after 259 nm LED illumination

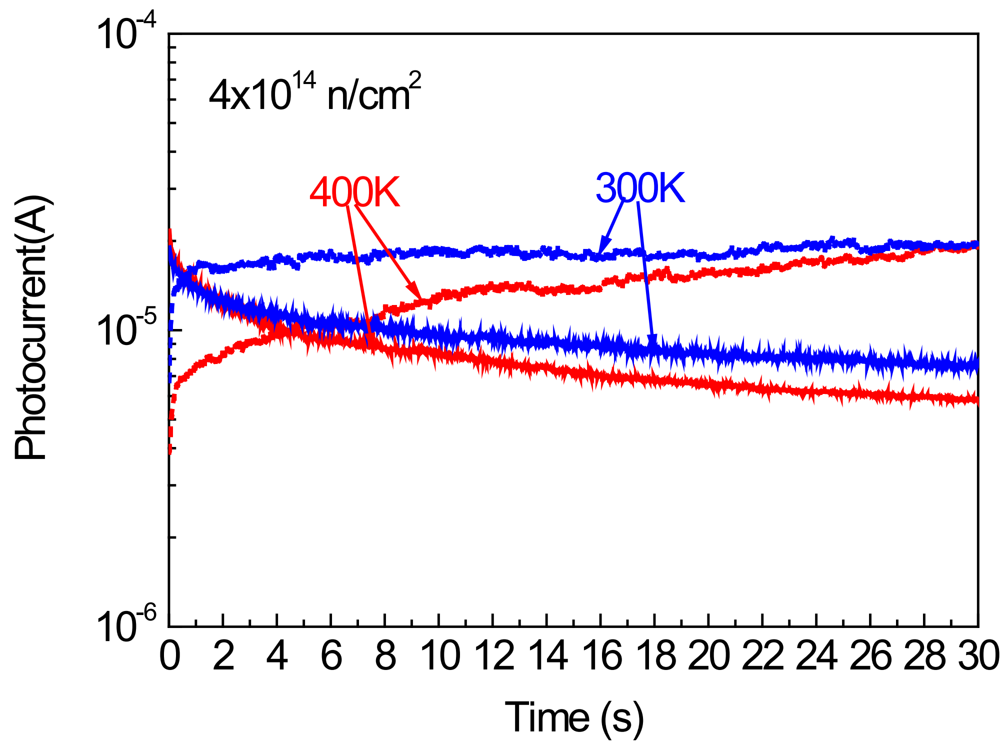

Fig. 6 (Color online) Photocurrent build-up and decay curves for 300K and 400K for sample S1_4E14

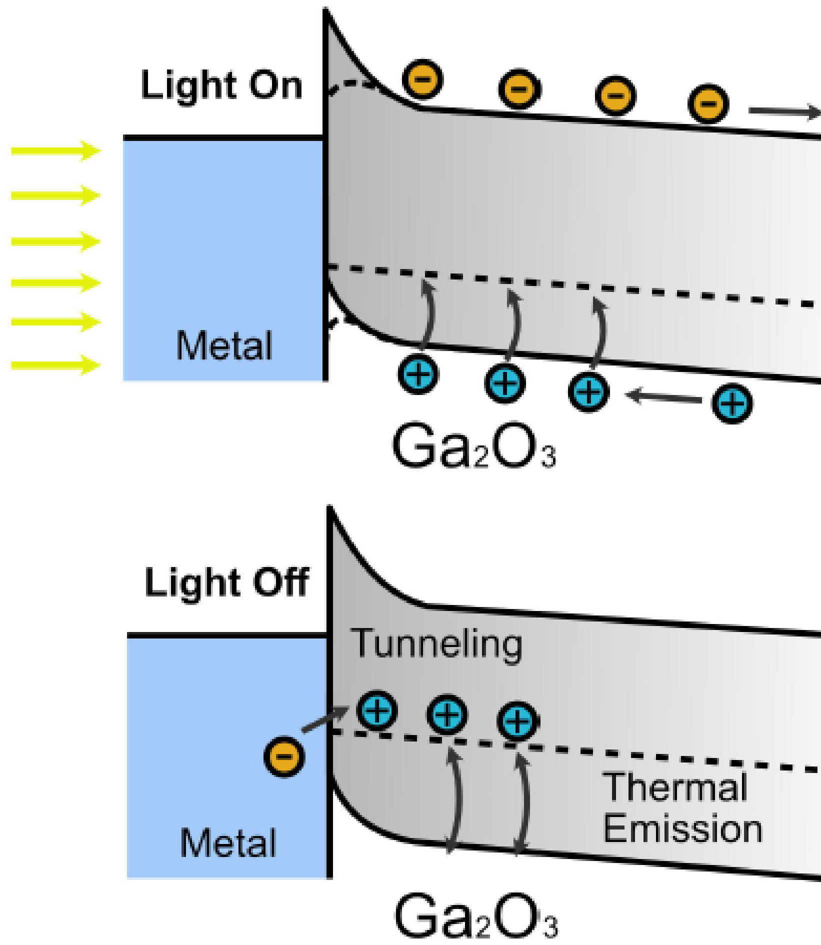

Fig.7 (Color online) Schematic representation of the processes involved in photocurrent build-up and decay in β-Ga_2O_3 Schottky diodes